doi:10.1016/j.jmb.2005.11.047 J. Mol. Biol. (2006) 355, 980–988

JMB

Available online at www.sciencedirect.com

SCIENCE DIRECT®

ELSEVIER

Crystal Structure of Human Guanosine Monophosphate Reductase 2 (GMPR2) in Complex with GMP

Jixi Li[1], Zhiyi Wei[2], Mei Zheng[1], Xing Gu[1], Yingfeng Deng[1], Rui Qiu[1] Fei Chen[1], Chaoneng Ji[1]*, Weimin Gong[2]*, Yi Xie[1] and Yumin Mao[1]

[1]*State Key Laboratory of Genetic Engineering, Institute of Genetics, School of Life Sciences, Fudan University Shanghai 200433, People's Republic of China*

[2]*National Laboratory of Biomacromolecules, Institute of Biophysics, Chinese Academy of Sciences, Beijing 100101 People's Republic of China*

**Corresponding authors*

Guanosine monophosphate reductase (GMPR) catalyzes the irreversible and NADPH-dependent reductive deamination of GMP to IMP, and plays a critical role in re-utilization of free intracellular bases and purine nucleosides. Here, we report the first crystal structure of human GMP reducatase 2 (hGMPR2) in complex with GMP at 3.0 Å resolution. The protein forms a tetramer composed of subunits adopting the ubiquitous $(\alpha/\beta)_8$ barrel fold. Interestingly, the substrate GMP is bound to hGMPR2 through interactions with Met269, Ser270, Arg286, Ser288, and Gly290; this makes the conformation of the adjacent flexible binding region (residues 268–289) fixed, much like a door on a hinge. Structure comparison and sequence alignment analyses show that the conformation of the active site loop (residues 179–187) is similar to those of hGMPR1 and inosine monophosphate dehydrogenases (IMPDHs). We propose that Cys186 is the potential active site, and that the conformation of the loop (residues 129–133) suggests a preference for the coenzyme NADPH over NADH. This structure provides important information towards understanding the functions of members of the GMPR family.

Keywords: guanosine monophosphate reductase 2; GMP; crystal structure; purine salvage

Introduction

Guanosine monophosphate (GMP) reductase (GMPR) (EC 1.6.6.8) plays an important role in the conversion of nucleoside and nucleotide derivatives of guanine (G) to adenine (A) nucleotides, and the maintenance of the intracellular balance between G and A nucleotides.[1] As one of the purine salvage enzymes, GMPR catalyzes the irreversible reductive deamination of GMP to IMP ($GMP+NADPH+H^+ \rightarrow IMP+NH_3+NADP^+$) and participates in the re-utilization of free intracellular bases and purine nucleosides.[2]

The GMP reductases exist in various organisms including *Tritrichomonas foetus*,[3] *Escherichia coli*,[4] *Bos taurus*,[5] and *Homo Sapiens*;[6] the amino acid sequence is similar across species. In humans, two isoenzymes of GMP reductase have been identified: hGMPR1 and hGMPR2.[7,8] The reaction mechanism and specificity of human GMPR1 were first reported in 1979.[7] At the amino acid level, hGMPR2 is 90% identical with hGMPR1, 93% identical with rat GMPR and 69% identical with *E. coli* GMPR. While hGMPR1 and hGMPR2 have different expression profiles in many tissues, the kinetic properties are quite similar: both exhibit a bimodal saturation curve and K_m values for substrates of hGMPR2 are in the same range as those reported for the purified erythrocyte enzyme hGMPR1.[8] In addition, for both isoenzymes NADPH is the preferred coenzyme and cannot be substituted by NADH or analogs of NADPH.[7,8]

In rats, GMPR has been shown to play a critical role in non-shivering thermogenesis, as evidenced by significant increases in expression in brown adipose tissue (BAT) during cold exposure. In the heat production response the role of BAT is to uncouple oxidative phosphorylation; therefore, GMPR may enhance uncoupling protein-1 (UCP-1) function by reducing inhibition of endogenous guanine nucleotides.[9] In humans, hGMPR2 has been shown to promote monocytic differentiation of HL-60 leukemia cells.[10]

Abbreviations used: GMPR, guanosine monophosphate reductase; hGMPR2, human GMPR2; IMPDH, inosine 5′-monophosphate dehydrogenase.

E-mail addresses of the corresponding authors: chnji@fudan.edu.cn; wgong@ibp.ac.cn

Inosine 5′-monophosphate dehydrogenase (IMPDH) has a reaction mechanism similar to that of GMPR, and as such is classified in the same set of purine salvage enzymes.[11] IMPDH catalyzes the conversion of IMP to xanthosine monophosphate (XMP); this is the rate-determining reaction in *de novo* guanine nucleotide biosynthesis, making IMPDH a drug design target for anticancer and immunosuppressive chemotherapy.[12] While hGMPR1 and hGMPR2 do not have significant amino acid similarity to human type I IMPDH or type II IMPDH,[8] hGMPR2 does show similarity (31% identity in their deduced amino acid sequences) to the IMPDH of *Borrelia burgdorferi*.[13] The crystal structure of IMPDH has been solved for many species,[13–18] which share similarities in active sites and geometry structures. Recently, the crystal structure of hGMPR1 was released in the Protein Data Bank†.

Here, we describe the crystal structure of human GMP reductase 2 in complex with GMP at 3.0 Å resolution to further our understanding of GMPR function in purine metabolism.

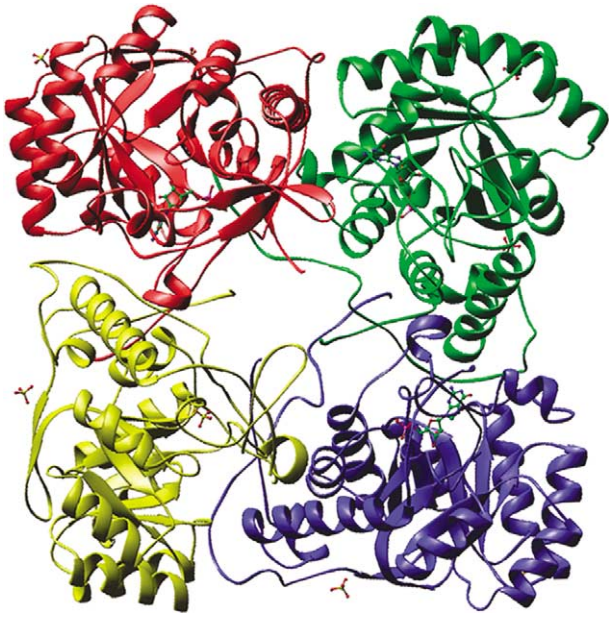

Figure 1. Ribbon diagram of human GMPR2 tetramer viewed along the 4-fold axis. Each monomer is shown in a different color.

Results and Discussion

Overall structure

The crystal structure of the hGMPR2 was refined to 3.0 Å resolution. The refined model consists of a homotetramer with dimensions of 85 Å×85 Å×50 Å, similar to *T. foetus*, hamster, and human type II IMPDH structures[14,15,19] (Figure 1). The monomers make contact along their edges, with α6 of one subunit close to the α8 of the next subunit, as well as along their N and C termini. These contacts may help stabilize the tetramer. The N and C termini of each monomer project from the bottom edge, forming a 25 Å×25 Å cavity in the tetramer along the *z* axis. The phosphate molecules are located on the surface of each subunit and have no interaction with the other subunits.

The monomer structure

Monomers A and B are composed of residues 1–338 (out of 348 amino acid residues), one GMP molecule, and two sulfate ions. Monomer C includes 327 amino acid residues (residues 1–278, 290–338), one GMP molecule, and two sulfate ions. Monomer D is composed of 317 amino acid residues (residues 1–267, 290–339) and two sulfate ions, but no GMP molecule. As little electron density was observed for one flexible region (residues 279–289 in C and residues 268–289 in D) and there was no observable electron density on the C-terminal residues 340–348 in any of the four subunits, these parts of the protein are disordered. In previous crystal structure studies of IMPDHs, these regions were also observed to be disordered.[14,15,19]

In the hGMPR2 structure, each monomer has a total of 11 α-helices and 14 β-sheets (Figure 2(a)), and forms an eight-stranded α/β barrel core with attached N and C-terminal sections. This barrel consists of eight sheets (β3∼β10) in parallel conformations, while β2 and β3 are located at the bottom of the barrel in antiparallel conformations. The other four β-sheets (β11–β14) are located between the barrel core and C terminus in antiparallel conformations.

The barrel core contains some hydrophilic residues that are highly conserved in the GMPR family. Asp219 and Met240, located on β9 and β10, respectively, form one hydrogen bond between the OD1 atom of Asp219 and SD atom of Met240 at a distance of 2.85 Å. The OD2 atom of Asp219 makes a hydrogen bond with the ND2 atom of Asn158 at a distance of 2.72 Å. Cys186 is hydrogen bonded to an O atom of Gly183 at a distance of 2.82 Å; these residues are both located in the proposed active site loop (residues 179–187). The OE1 atom of Glu118 forms two hydrogen bonds with the NH1 and NH2 atoms of Arg148 at distances of 2.52 Å and 2.92 Å, respectively. These residues provide a hydrophilic surrounding that may make the α/β barrel more stable and the substrate more suitable for the active site pocket.

Disulfide bonds play a key role in stabilizing protein tertiary structures;[20] the formation of disulfide bond is particularly important for the proper folding of secreted proteins in various organisms.[21] It was observed that a disulfide bond is formed in hGMPR2 between residues Cys68 and

† http://www.rcsb.org/pdb

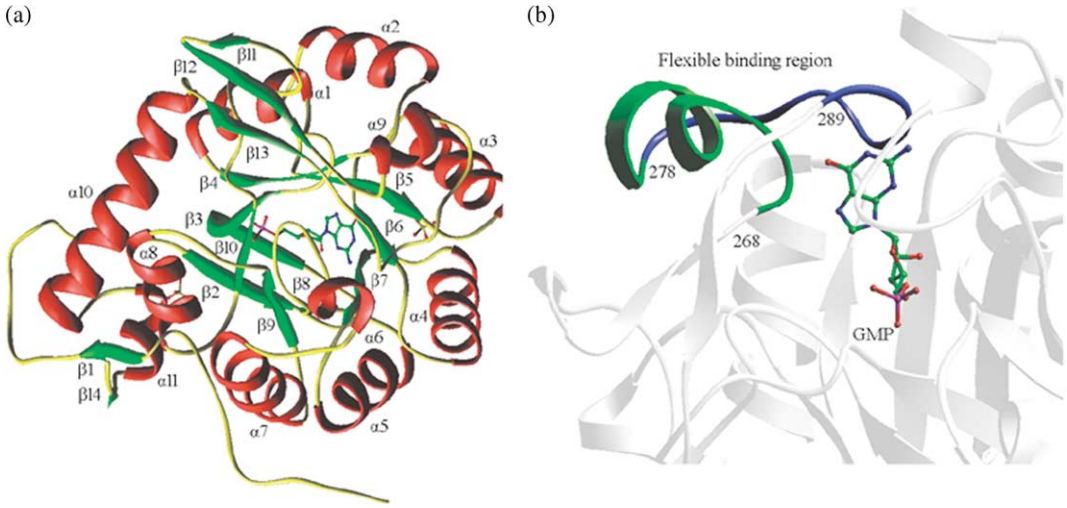

Figure 2. (a) Ribbon representation of one monomer structure of human GMPR2, showing 11 α-helices and 14 β-sheets. An $(\alpha/\beta)_8$ barrel is formed from β3 to β10. (b) The disordered region (residues 268–278) both in subunit C and D is colored with blue, and in subunit D another disordered region (residues 279–289) is colored green. The GMP molecule is shown as a ball-and-stick model.

Cys95, which are located in α1 and the loop between α2 and β5, respectively. Cys68 and Cys95 are not conserved in the GMPR and IMPDH families; while the disulfide bond is not common in the GMPR family, it may still be important for stabilization of the tetramer.

Substrate binding and conformation change

Interestingly, it was observed that the GMP molecule binds to the monomers A, B, and C, but not D, which may be the result of partial binding of GMP molecules to hGMPR2. In monomers A, B, and C, the substrate GMP is located on the top of the barrel, surrounded by a hydrophilic surface formed by the active site loop (residues 179–187) and the flexible binding region (residues 268–290). The guanine and phosphate moieties of GMP make a number of protein interactions with the adjacent residues (Figure 3(a)). The N1 and N2 atoms of the guanine ring make hydrogen bonds with Ser288, the N7 atom with Met269 and the O6 atom with Ser270 and Gly290. The ribose interacts with Asp219 and Arg286 through the network of hydrogen bonds. The phosphate group is anchored in place by four amino acid main-chain nitrogen atoms (Ser184, Gly221, Gly242, and Gly243) (Figure 3(b)). These observed bonds are consistent with the corresponding residues shown to interact with IMP in IMPDHs.[14–18] Most of the previously listed interactions are highly conserved in GMPRs and IMPDHs, with the exception that Gly242 is substituted for Ser, Asn, or Arg in IMPDHs.[14–18]

While the GMP binding loop is flexible in hGMPR2 monomers, we found that the conformation changed along with the binding level of GMP (Figure 4). In monomers A and B, electrical density can be clearly observed, and GMP interacts tightly with the binding loop. In monomer C, the binding loop was partly disordered (residues 279–289). Unlike that in monomer A, the O6 atom of the guanine ring did not make hydrogen bonds with Ser270 and Gly290. It can be concluded that the GMP bound these residues loosely. No GMP binding was seen with monomer D, and the disordered region (residues 268–289) was longer than that in monomer C (Figure 2(b)). Therefore, it is reasonable to postulate the following mechanism for how the substrate GMP interacts with hGMPR2: the flexible binding loop, located on the top of the barrel, is like a door on a hinge. The loop closes when the GMP enters the barrel, or it would be opened with flexible conformation.

Xanthosine monophosphate (XMP) is reported to be a competitive inhibitor with respect to GMP, and a non-competitive inhibitor with respect to NADPH.[7,8] 6-ThioGMP, 6-thioIMP, and 6-chloropurine ribonucleotide caused apparent inactivation of GMPR.[7] Since GMP and XMP are similar in the molecular structure and space volume, we suggest that inhibitor XMP may hold the GMP binding space and form hydrogen bonds with the corresponding hydrophilic residues, Ser184, Asp219, Arg286 and so on.

Comparison of hGMPR2, hGMPR1, and IMPDHs

HGMPR2, hGMPR1, and IMPDHs share the same $(\alpha/\beta)_8$-barrel fold, which is the most common fold among proteins.[22] While hGMPR2 and hGMPR1 have different tissue expression profiles, their overall structures are almost identical. The GMP binding sites are highly conserved in the GMPR family and the conformation of GMP in hGMPR2 is similar to that in the complex crystal of hGMPR1 (PDB ID: 2BLE), which provides evidence for the consistency of enzymic property between hGMPR2 and hGMPR1.[7,8]

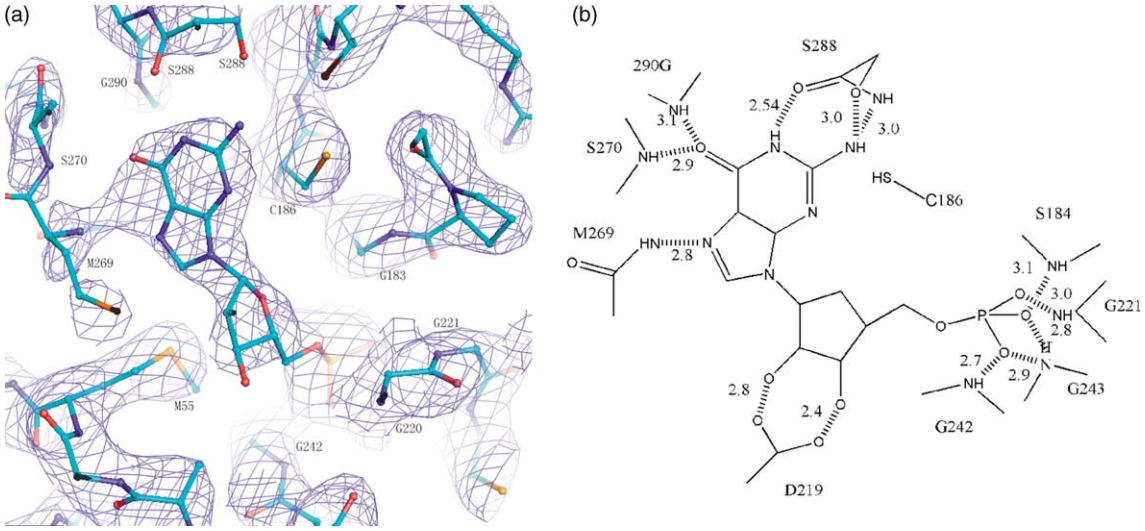

Figure 3. (a) Ball-and-stick model of the electron density map ($2F_o - F_c$, 1σ) of GMP with adjacent residues labeled. The GMP molecule and the residues are shown in a ball-and-stick model. (b) Cartoon representation of bound GMP, showing side-chain interactions.

The sequence alignment of GMPRs from different organisms and seven IMPDH proteins (PDB codes 2BLE, 1VRD, 1EEP, 1ZFJ, 1JR1, 1NFB, 1JCN, and 1PVN) is shown in Figure 5. The alignment reveals an IMP dehydrogenase/GMP reductase domain between residues 88 and 342, which covers ten α-helices and ten β-sheets in hGMPR2. While human GMPR2 shares only about 30% identity with IMPDHs, the results of RMSD values between hGMPR2 and IMPDH family members with 268 aligned residues by the multi-structure alignment analysis (1VRD:A, 1.633; 1EEP:A, 1.601; 1ZFJ:A, 1.441; 1JR1:A, 1.673; 1NFB:A, 1.757; 1JCN:A, 1.768; 1PVN:A, 1.674) suggest that they adopt a similar structure and may have a similar catalytic mechanism. The catalytic site residues Asp129, Ser135, Gln158, Asp174, Ser184, Cys186, Thr188, Gln198, and Asp219 are conserved between GMPRs and IMPDHs.

The main differences between hGMPR2 and IMPDHs lie in the regions 93–99 and 179–187, as well as the N and C-terminal tails. The orientation of the proposed active site loop (179–187), which acts as a functional lid during catalysis, is similar to those in some IMPDHs, but subtly different from that in *B. burgdorferi* IMPDH.[13–18] In addition, the location of the β2-sheet is different: it is far away from the active site and may have no contribution to the catalytic activity. Finally, while three hydrophilic residues, Ser102, Ser103, and Cys222, are identical in the GMPR family, the corresponding sites in IMPDHs contain hydrophobic residues.

Structural comparison and model construction were employed to investigate the interaction between substrate NADPH and hGMPR2. One significant difference is that the conformation of the loop (residues 129–133) in hGMPR2 is shifted 3.7 Å relative to those of IMPDHs (Figure 6).

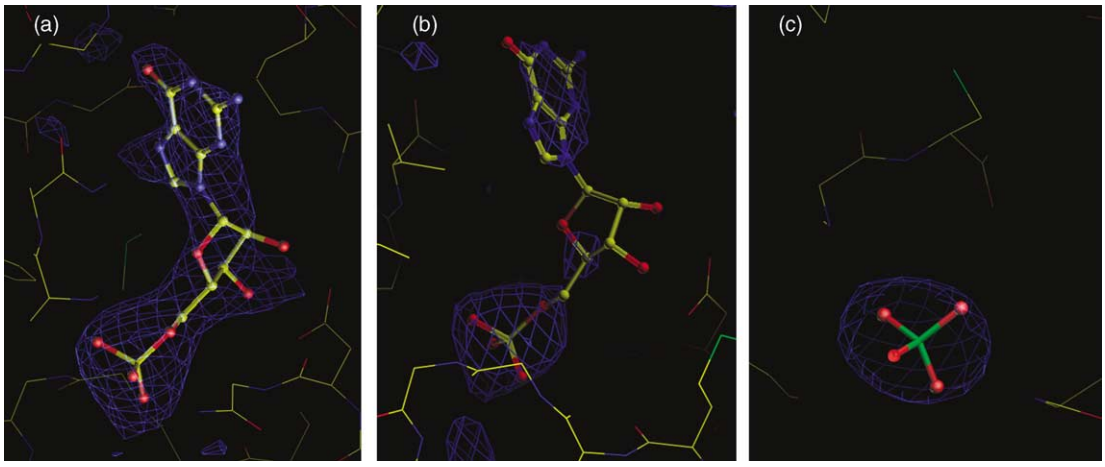

Figure 4. The GMP structure shown with an annealed composite omit electron density map ($F_o - F_c$) at 2.5σ. (a) GMP in monomer A and B; (b) GMP in monomer C; (c) one sulfate ion occupied part of the GMP binding site in monomer D.

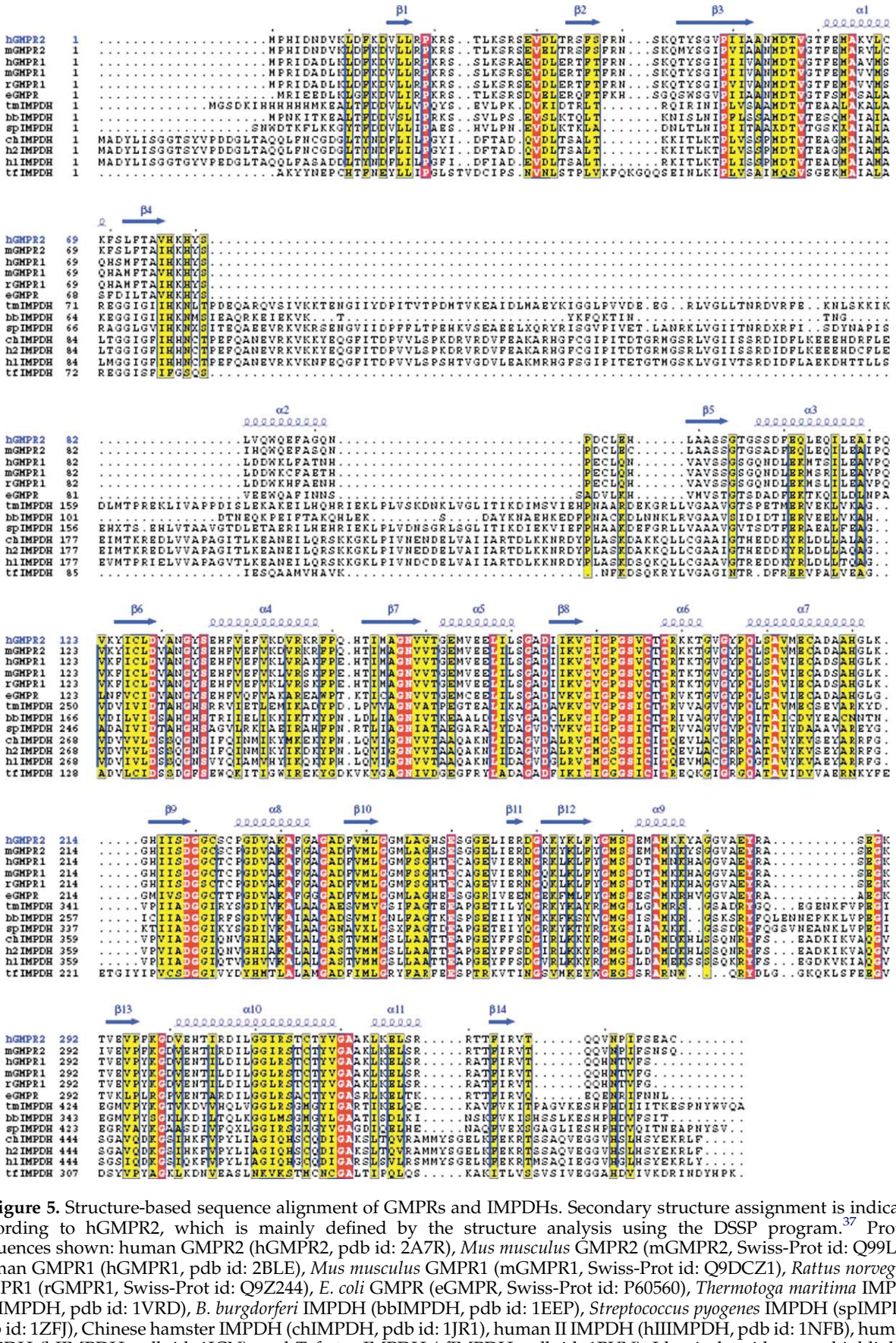

Figure 5. Structure-based sequence alignment of GMPRs and IMPDHs. Secondary structure assignment is indicated according to hGMPR2, which is mainly defined by the structure analysis using the DSSP program.[37] Protein sequences shown: human GMPR2 (hGMPR2, pdb id: 2A7R), *Mus musculus* GMPR2 (mGMPR2, Swiss-Prot id: Q99L27), human GMPR1 (hGMPR1, pdb id: 2BLE), *Mus musculus* GMPR1 (mGMPR1, Swiss-Prot id: Q9DCZ1), *Rattus norvegicus* GMPR1 (rGMPR1, Swiss-Prot id: Q9Z244), *E. coli* GMPR (eGMPR, Swiss-Prot id: P60560), *Thermotoga maritima* IMPDH (tmIMPDH, pdb id: 1VRD), *B. burgdorferi* IMPDH (bbIMPDH, pdb id: 1EEP), *Streptococcus pyogenes* IMPDH (spIMPDH, pdb id: 1ZFJ), Chinese hamster IMPDH (chIMPDH, pdb id: 1JR1), human II IMPDH (hIIIMPDH, pdb id: 1NFB), human I IMPDH (hIIMPDH, pdb id: 1JCN), and *T. foetus* IMPDH (tfIMPDH, pdb id: 1PVN). Identical residues are highlighted with red boxes; those that are similar are shown in yellow boxes.

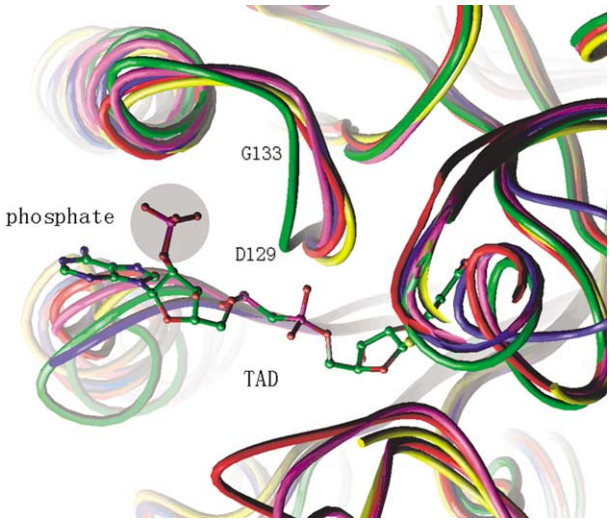

Figure 6. Detailed comparison between hGMPR2 and IMPDHs. hGMPR2 (green), *Streptococcus pyogenes* IMPDH (red), *B. burgdorferi* IMPDH (blue), *T. foetus* IMPDH (yellow) and hamster IMPDH (purple). β-Me-TAD is shown at the active site as a ball-and-stick model. The dummy phosphate group was added to the AO2 atom of TAD with a shaded circle. The residues Asp129 and Gly133 in the loop are listed.

Surprisingly, insertion of the IMP inhibitor β-Me-TAD into the corresponding position in hGMPR2 moves the loop closer to the position IMPDH bound with NADH.[15] Although NADPH has one more phosphate moiety than NADH, there is a Tris group in IMPDH close to where β-Me-TAD is bound,[15] which makes the space larger and more suitable for the catalysis of IMPDH. In addition, residues in the loop (129–133) of hGMPR2 can interact with NADPH, which may explain the marked preference of GMPR for NADPH as the coenzyme over NADH or analogues of NADPH.[7,8] At the active site flap, Ser270 is highly flexible and disordered in monomer D of hGMPR2 as well as several IMPDHs.[14–16] Ser270 is identical in the GMPR family, while substituted by Gly in IMPDHs, and may interact with the phosphate moiety of NADPH to provide a suitable surrounding for substrate binding.

Proposed active site loop

GMPR and IMPDH were identified to belong to the same set of purine salvage enzymes due to their similarities in reaction mechanism. The mechanism for the catalytic reaction of IMPDH has been clearly elucidated in the hamster:[23] first, the sulfur atom of Cys331 forms a covalent bond with the C2 carbon atom of IMP to yield an oxidized IMP thioimidate intermediate (XMP*),[14] which can also form a covalent bond with the inhibitor 6-Cl IMP. NADH is then released; finally, the bond to the product is broken and XMP is released. Human GMPR2 has similar overall topology to the active sites of known structures of IMPDHs.[13–18,23] The binding sites of GMP in hGMPR2 are identical with those in IMPDHs.[13–18,23] Cys186 has previously been identified as a key residue in catalysis, and is highly conserved in the IMPDH family.[13–18,24–26] And in hGMPR2, the enzyme activity of mutant Cys186 to alanine was less than 5% of the wild-type level (data shown in Appendix). Therefore, Cys186 is proposed as the active site for catalyzing reaction. Moreover, the amino acid residues of the active loop (residues 179–187) are highly conserved in GMPR and IMPDH families. This active site loop appears to move like a door on a hinge but can also assume other conformations.[14–17] The similar active-site geometry supports the observation that both GMPR and IMPDH bind substrate GMP before cofactor NADPH.[7]

Conclusions

We have determined the crystal structure of human GMP reducatase 2 (hGMPR2) at 3.0 Å resolution: the protein forms a tetramer consisting of subunits adopting the ubiquitous $(\alpha/\beta)_8$ barrel fold. Interestingly, the substrate GMP binds hGMPR2 through interaction with a number of amino acids, fixing the conformation of the flexible binding region (residues 268–289). Structural comparison and sequence alignment analyses show the conformation of the active site loop (residues 179–187) to be similar to those of hGMPR1 and IMPDHs. We propose that Cys186 is the potential active site, and that the conformation of the loop (residues 129–133) markedly prefers NADPH to NADH. This work provides insights into the structure and function of the GMPR family, and may aid understanding of the reaction mechanisms of GMPRs in the future.

Methods

Crystallization and data collection

Human GMPR2 was expressed from the pQE31 vector in *E. coli* M15 cells; the protein was purified by affinity chromatographic and crystallized as described earlier.[27] Diffraction data were collected on an ADSC Quantum 4R detector on beamline 18B at the Photon Factory in Japan as well as a Mar-CCD detector on beamline 3W1 at the Beijing Synchrotron Radiation Facility, Institute of High Energy Physics, Chinese Academy of Science.

Molecular replacement and refinement

The crystal structure was solved through the molecular replacement method using the 1.9 Å resolution structure of human GMPR1 as a search model (Protein Data Bank entry 2BLE). Subsequent model building and refinement were carried out using programs CCP4i[28] and CNS.[29] The non-crystallographic symmetry restraint was applied to improve the model refinement with the help of the *R*-free factor. Manual adjustments were used to rebuild the model, using the program O[30] as well as $2F_o - F_c$ and

Table 1. Statistics for data collection and refinement

Unit cell (Å, deg.)	
a, b (Å)	110.6
c (Å)	209.8
α, β (deg.)	90
γ (deg.)	120
Resolution limit (Å)	20–3 (3.16–3)
Completeness (%)	100 (100)
No. reflections	483,679
No. independent reflections	29,287
R_{merge} (%)	0.089(0.189)
I/σ	7.3(3.2)
R_{work}(%)[a]	22.8
R_{free}(%)[b]	27.6
GMP molecules	3
Sulfate ion	8
Water molecules	12
Overall *B*-factor (Å^2)	52.3
Stereochemistry (r.m.s.deviation)	
Bond lengths (Å)	0.009
Bond angles (deg.)	1.4

[a] $R_{work} = \Sigma||F_{obs}|-|F_{calc}||/\Sigma|F_{obs}|$, where F_{obs} and F_{calc} are observed and calculated structure factors.

[b] $R_{free} = \sum_T ||F_{obs}|-|F_{calc}||/\sum_T |F_{obs}|$, where T is a test data set of 10% of the total reflections randomly chosen and set aside prior to refinement.

F_o-F_c electron density maps as references. For each of the monomers, two peaks (above 3δ) in the F_o-F_c electron density map were found at the surface of the monomer. These peaks were defined as sulfate ions, as both Li_2SO_4 and $(NH_4)_2SO_4$ are present in the protein solution and the electronic density fits well with a sulfate ion. The final *R*-factor is 22.8% with an *R*-free of 27.6% for all reflections between 20 Å and 3 Å resolution. The stereo-chemical quality of the final model was checked by PROCHECK,[31] and the final refinement statistics and geometry were very good (Table 1).

Structure analysis and comparison

GMPR and IMPDH sequences were identified in the sequence data bank using BLAST.[32] The alignment of multiple sequences was performed with CLUSTAL W.[33] The program SSM was used to perform the multi-structure alignment.[34] The diagrams in Figures 1, 2, and 6 were carried out using the program Ribbons.[35] Figures 3 and 4 were made using program O.[30] Figure 5 was produced using the program ESPript.[36]

Protein Data Bank accession codes

The atomic coordinates and structure factors (code 2A7R) have been deposited in the Protein Data Bank, Research Collaboratory for structural Bioinformatics, Rutgers University, New Brunswick, NJ†.

Acknowledgements

We thank Christina A. Doyle of Columbia University and Enpeng Zhao of the University of Wisconsin-Madison for critical reading of the manuscript. This work is supported by the National Natural Science Foundation of China (grant no. 30470355 and 10490193) and the CNHLPP Project (973) of China (grant no. 2004CB520801).

Supplementary Data

Supplementary data associated with this article can be found, in the online version, at doi:10.1016/j.jmb.2005.11.047

Appendix

Mutagenesis, measurement of enzyme activity

A mutation was made in human GMPR2 cDNA cloned into a pBluescript II SK (+) vector by a four-primer polymerase chain reaction (PCR) method using Pfu DNA polymerase. PCR products were digested with restriction enzymes KpnI and HindIII, and cloned into pQE31 vector (Qiagen). After sequencing, the right mutants of GMPR2 were transformed into *E. coli* M15 cells. After induction with IPTG, the GMPR2 fusion protein was purified with affinity chromatography as described by Deng *et al*.[27] The purified protein was dialyzed against the stock buffer containing 5 mM Tris–HCl (pH 8.0) and 50% glycerol. The purified protein was stored at −20 °C until used.

For assay of GMP reductase activity, the reduction of GMP was monitored by following the concomitant oxidation of NADPH at 340 nm on an Ultrospec 4000 spectrophotometer (Pharmacia). The reaction mixture contained 50 mM Tris–HCl (pH 7.8), 2 mM 2-mercaptoethanol, 1 mM EDTA, 0.1 mM NADPH, 0.1 mM GMP and 8 μg of purified GMPR2 per 0.5 ml of reaction mixture. Reactions were initiated with enzyme subsequent to

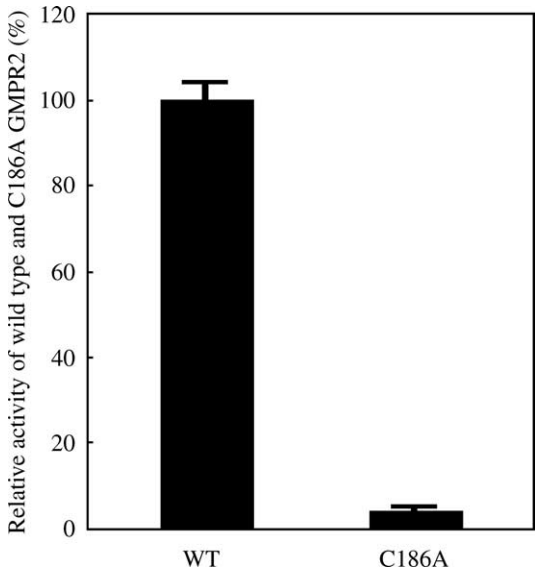

Figure 7. Mutational analysis of the proposed active site. The enzymatic activity of wild-type or mutants of hGMPR2 were obtained at 340 nm at 37 °C.

pre-incubation for 10 min at 37 °C without GMP or NADPH.

We generated one mutant to explore the roles of the proposed hGMPR2 active site residue Cys186 in catalysis (Figure 7). The enzyme activity of mutant Cys186 to alanine was less than 5% of the wild-type level. So, the C186A mutant primarily supports the hypothesis that Cys186 is the catalytic active site.

References

1. Neuhard, J. & Nygaard, P. (1987). Purines and Pyrimidines. In Escherichia coli *and* Salmonella typhimurium Cellular and Molecular Biology (Neidhardt, F. C., Ingraham, J. L., Low, K. B., Magasanik, B., Schaechter, M. & Umbarger, E., eds), vol. 1, pp. 445–473, American Society for Microbiology, Washington, DC.
2. Berens, R. L., Krug, E. C. & Marr, J. J. (1995). In *Biochemistry and Molecular Biology of Parasites* (Marr, J. J. & Muller, M., eds), pp. 89–117, Academic Press, London.
3. Beck, J. T., Zhao, S. & Wang, C. C. (1994). Cloning, sequencing and structural analysis of the DNA encoding inosine monophosphate dehydrogenase (EC 1.1.1.205) from *Tritrichomonas foetus*. *Expt. Parasitol.* **78**, 101–112.
4. Andrews, S. C. & Guest, J. R. (1988). Nucleotide sequence of the gene encoding the GMP reductase of *Escherichia coli* K12. *Biochem. J.* **255**, 35–43.
5. Stephens, R. W. & Whittaker, V. K. (1973). Calf thymus GMP reductase: control by XMP. *Biochem. Biophys. Res. Commun.* **53**, 975–981.
6. Mackenzie, J. J. & Sorensen, L. B. (1973). Guanosine 5′-phosphate reductase of human erythrocytes. *Biochem. Biophys. Acta*, **327**, 282–294.
7. Spector, T., Jones, T. E. & Miller, R. L. (1979). Reaction mechanism, and specificity of human GMP reductase: substrates, inhibitors, activators and inactivators. *J. Biol. Chem.* **254**, 2308–2315.
8. Deng, Y., Wang, Z., Ying, K., Gu, S., Ji, C., Huang, Y. *et al*. (2002). NADPH-dependent GMP reductase isoenzyme of human (GMPR2): expression, purification, and kinetic properties. *Int. J. Biochem. Cell Biol.* **34**, 1035–1050.
9. Salvatore, D., Bartha, T. & Larsen, P. R. (1998). The guanosine monophosphate reductase gene is conserved in rats and its expression increases rapidly in brown adipose tissue during cold exposure. *J. Biol. Chem.* **273**, 31092–31096.
10. Zhang, J., Zhang, W., Zou, D., Chen, G., Wan, T., Zhang, M. & Cao, X. (2003). Cloning and functional characterization of GMPR2, a novel human guanosine monophosphate reductase, which promotes the monocytic differentiation of HL-60 leukemia cells. *J. Cancer Res. Clin. Oncol.* **129**, 76–83.
11. Becerra, A. & Lazcano, A. (1998). The role of gene duplication in the evolution of purine nucleotide salvage pathways. *Orig. Life Evol. Biosph.* **28**, 539–553.
12. Markham, G. D., Bock, C. L. & Schalk-Hihi, C. (1999). Acid-base catalysis in the chemical mechanism of inosine monophosphate dehydrogenase. *Biochemistry*, **38**, 4433–4440.
13. McMillan, F. M., Cahoon, M., White, A., Hedstrom, L., Petsko, G. A. & Ringe, D. (2000). Crystal structure at 2.4 Å resolution of *Borrelia burgdorferi* inosine 5′-monophosphate dehydrogenase: evidence of a substrate-induced hinged-lid motion by loop 6. *Biochemistry*, **39**, 4533–4542.
14. Sintchak, M. D., Fleming, M. A., Futer, O., Raybuck, S. A., Chambers, S. P., Caron, P. R. *et al*. (1996). Structure and mechanism of inosine monophosphate dehydrogenase in complex with the immunosuppressant mycophenolic acid. *Cell*, **85**, 921–930.
15. Gan, L., Petsko, G. A. & Hedstrom, L. (2002). Crystal structure of a ternary complex of *Tritrichomonas foetus* inosine 5′-monophosphate dehydrogenase: NAD+ orients the active site loop for catalysis. *Biochemistry*, **41**, 13309–13317.
16. Gan, L., Seyedsayamdost, M. R., Shuto, S., Matsuda, A., Petsko, G. A. & Hedstrom, L. (2003). The immunosuppressive agent mizoribine monophosphate forms a transition state analogue complex with inosine monophosphate dehydrogenase. *Biochemistry*, **42**, 857–863.
17. Zhang, R., Evans, G., Rotella, F. J., Westbrook, E. M., Beno, D., Huberman, E. *et al*. (1999). Characteristics and crystal structure of bacterial inosine-5′-monophosphate dehydrogenase. *Biochemistry*, **38**, 4691–4700.
18. Whitby, F. G., Luecke, H., Kuhn, P., Somoza, J. R., Huete-Perez, J. A., Phillips, J. D. *et al*. (1997). Crystal structure of *Tritrichomonas foetus* inosine-5′-monophosphate dehydrogenase and the enzyme–product complex. *Biochemistry*, **36**, 10666–10674.
19. Colby, T. D., Vanderveen, K., Strickler, M. D., Markham, G. D. & Goldstein, B. M. (1999). Crystal structure of human type II inosine monophosphate dehydrogenase: implications for ligand binding and drug design. *Proc. Natl Acad. Sci. USA*, **96**, 3531–3536.
20. Hiniker, A. & Bardwell, J. C. (2003). Disulfide bond isomerization in prokaryotes. *Biochemistry*, **42**, 1179–1185.
21. Molinari, M. & Helenius, A. (1999). Glycoproteins form mixed disulphides with oxidoreductases during folding in living cells. *Nature*, **402**, 90–93.
22. Nagano, N., Orengo, C. A. & Thornton, J. M. (2002). One fold with many functions: the evolutionary relationships between TIM barrel families based on their sequences, structures and functions. *J. Mol. Biol.* **321**, 741–765.
23. Prosise, G. L. & Luecke, H. (2003). Crystal structures of *Tritrichomonas foetus* inosine monophosphate dehydrogenase in complex with substrate, cofactor and analogs: a structural basis for the random-in ordered-out kinetic mechanism. *J. Mol. Biol.* **326**, 517–527.
24. Gan, L., Seyedsayamdost, M. R., Shuto, S., Matsuda, A., Petsko, G. A. & Hedstrom, L. (2003). The immunosuppressive agent mizoribine monophosphate forms a transition state analogue complex with inosine monophosphate dehydrogenase. *Biochemistry*, **42**, 857–863.
25. Huete-Perez, J. A., Wu, J. C., Whitby, F. G. & Wang, C. C. (1995). Identification of the IMP binding site in the IMP dehydrogenase from *Tritrichomonas foetus*. *Biochemistry*, **34**, 13889–13894.
26. Antonino, L. C., Straub, K. & Wu, J. C. (1994). Probing the active site of human IMP dehydrogenase using halogenated purine riboside 5′-monophosphates and covalent modification reagents. *Biochemistry*, **33**, 1760–1765.

27. Ji, C. N., Ying, G., Deng, Y. F., Chen, S., Zhang, W. H., Shu, G. *et al*. (2003). Purification, crystallization and preliminary X-ray studies of GMP reductase 2 from human. *Acta Crystallog. sect. D*, **59**, 1109–1110.
28. Potterton, E., Briggs, P., Turkenburg, M. & Dodson, E. (2003). A graphical user interface to the CCP4 program suite. *Acta Crystallog. sect. D*, **59**, 1131–1137.
29. Brunger, A. T., Adams, P. D., Clore, G. M., DeLano, W. L., Gros, P., Grosse-Kunstleve, R. W. *et al*. (1998). Crystallography & NMR system: a new software suite for macromolecular structure determination. *Acta Crystallog. sect. D*, **54**, 905–921.
30. Leslie, A. G. W. (1994). *MOSFLM User Guide*, MRC-LMB, Cambridge.
31. Laskowski, R., Macarthur, M., Moss, D. & Thornton, J. (1993). Procheck—a program to check stereochemical quality of protein structures. *J. Appl. Crystallog.* **26**, 283–290.
32. Altschul, S. F., Madden, T. L., Schaffer, A. A., Zhang, J., Zhang, Z., Miller, W. & Lipman, D. J. (1997). Gapped BLAST and PSI-BLAST: a new generation of protein database search programs. *Nucl. Acids Res.* **25**, 3389–3402.
33. Thompson, J. D., Higgins, D. G. & Gibson, T. J. (1994). CLUSTAL W.: improving the sensitivity of progressive multiple sequence alignment through sequence weighting, position-specific gap penalties and weight matrix choice. *Nucl. Acids Res.* **22**, 4673–4680.
34. Krissinel, E. & Henrick, K. (2004). Secondary-structure matching (SSM), a new tool for fast protein structure alignment in three dimensions. *Acta Crystallog. sect. D*, **60**, 2256–2268.
35. Carson, M. (1997). Ribbons. *Methods Enzymol.* **277**, 493–505.
36. Gouet, P., Courcelle, E., Stuart, D. I. & Metoz, F. (1999). ESPript: analysis of multiple sequence alignments in PostScript. *Bioinformatics*, **15**, 305–308.
37. Kabsch, W. & Sander, C. (1983). *Biopolymers*, **22**, 2577–2637.

Edited by R. Huber

(Received 11 July 2005; received in revised form 4 November 2005; accepted 15 November 2005)
Available online 1 December 2005